ELECTRONS IN SOLIDS

Small mass → small momentum p → large de Broglie wavelength λ

$\lambda = h/p = 2\pi/k$

wavevector $k = \hbar p$ *(e.g., plane wave is* Ae^{ikr}*)*

$$\lambda(\mathring{A}) = \sqrt{\frac{150}{E(eV)}}$$

For low energy electrons, comparable or larger than distance between atoms (scattering centers). Hence, cannot use concept of classical trajectories.

Long wavelength → strong diffraction
→ spill over barriers

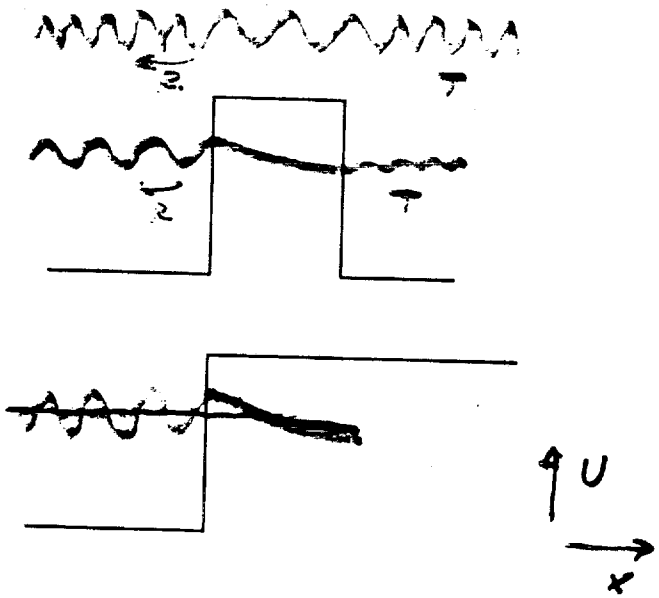

Interference and diffraction

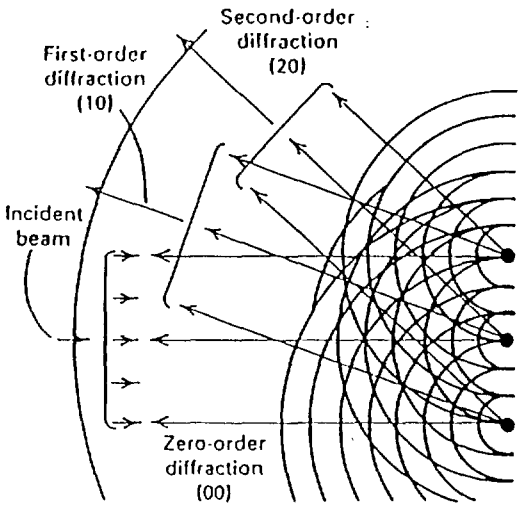

LOW ENERGY ELECTRON DIFFRACTION (LEED)

Crystalline lattice produce diffraction spots.

Sampling depth is short (1-3 monolayers) if one chooses those electrons that did not interact inelastically (elastic scattered).

Analysis of spots serve to determine symmetry of substrate surface and adsorbates, reconstruction, etc.

Measurements of spot intensity plus computer modeling can give information about atom location at surfaces.

Difference with X-ray diffraction in that scattering is strong. Thus kinematic theory is insufficient, dynamic theory needed.

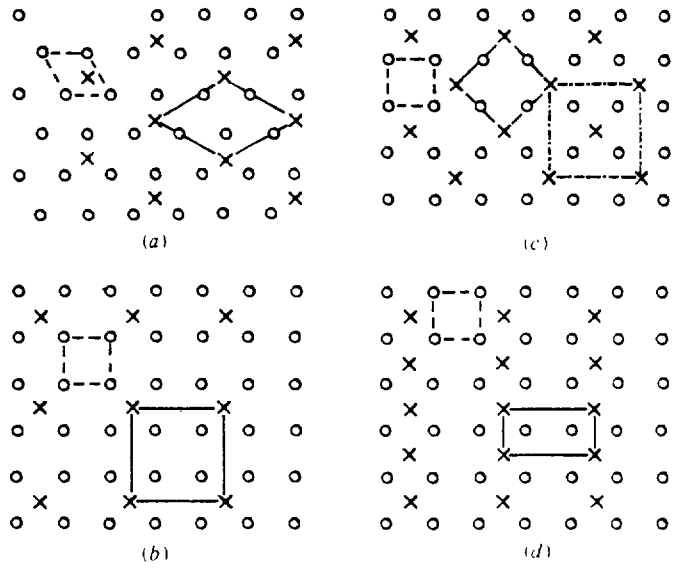

Fig. 2.5 Examples of overlayer structures in which the open circles represent the periodicity of the substrate while the crosses show adsorbate or selvedge mesh periodicity. In each case the substrate Bravais net is shown dashed while the full surface Bravais net is shown with full lines. (*a*) shows a $(\sqrt{3} \times \sqrt{3})R30°$ structure on an hexagonal substrate, the matrix notation being $\begin{pmatrix} 2 & 1 \\ -1 & 1 \end{pmatrix}$. (*b*), (*c*) and (*d*) show (2×2) or $\begin{pmatrix} 2 & 0 \\ 0 & 2 \end{pmatrix}$, $(\sqrt{2} \times \sqrt{2})R45°$ or $\begin{pmatrix} 1 & 1 \\ -1 & 1 \end{pmatrix}$ and (2×1) or $\begin{pmatrix} 2 & 0 \\ 0 & 1 \end{pmatrix}$, structures. Note in case (*c*) that the dash–dot net is centred but not rotated relative to the substrate unit mesh so that this structure is often referred to as $c(2 \times 2)$, necessitating the notation $p(2 \times 2)$ for structure (*b*).

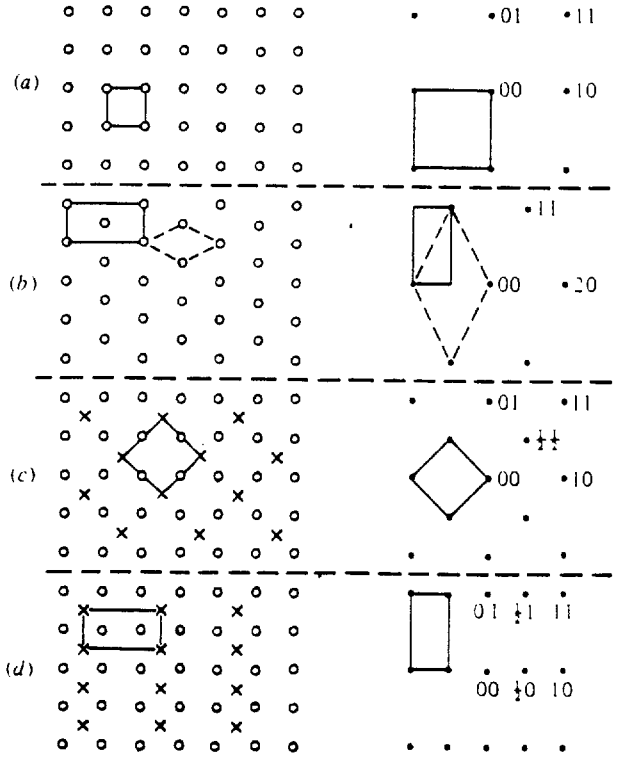

Fig. 2.7 Some real and reciprocal meshes, the relevant unit meshes being marked. Reciprocal net points are also labelled using the convention described in the text. Note that examples (*a*) and (*b*) represent unreconstructed surfaces while (*c*) and (*d*) show an adsorbate or selvedge structure (crosses) superimposed on a substrate structure (circles). In (*b*) the *primitive* real and reciprocal unit nets are shown dashed.

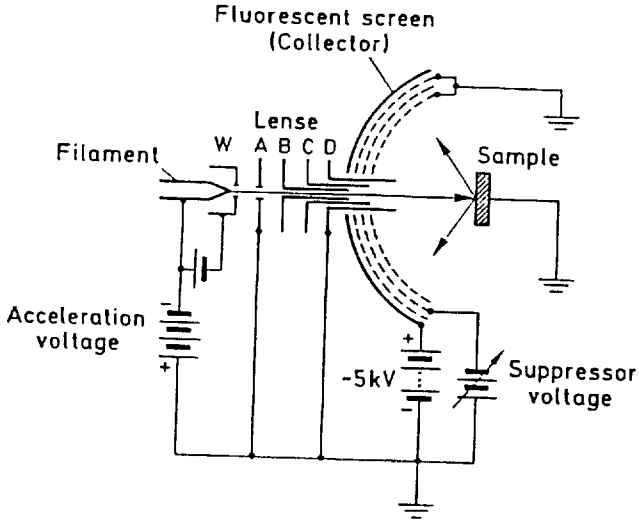
Fluorescent screen
(Collector)
Lense
W A B C D
Filament
Sample
Acceleration
voltage
-5kV
Suppressor
voltage

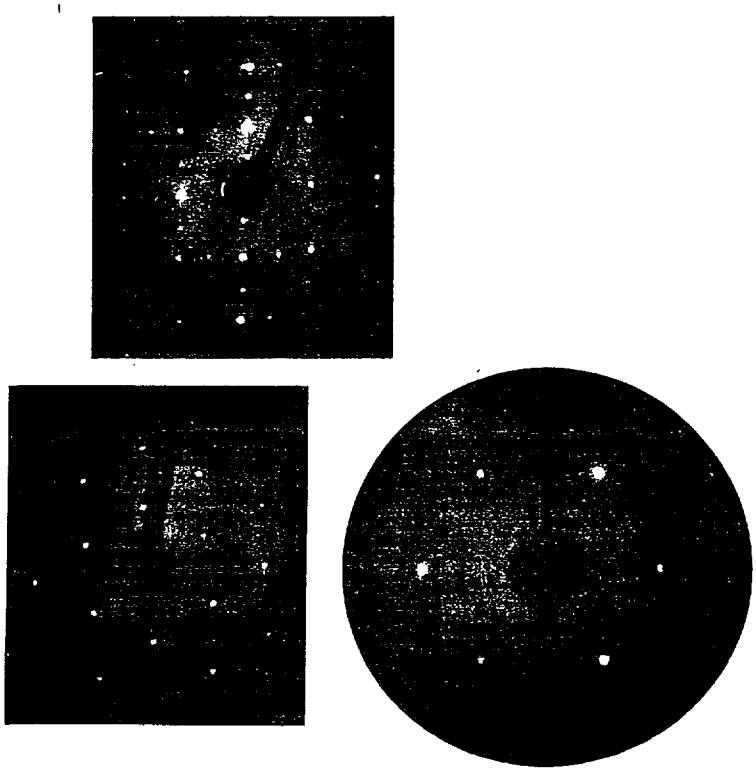

REVERSE VIEW LEED
MODEL RVL 8-120

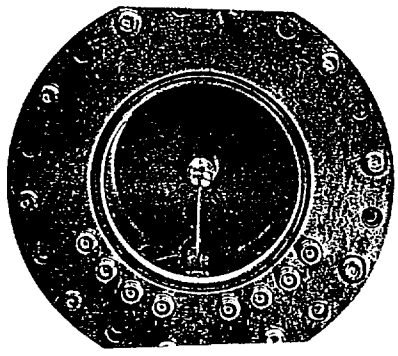

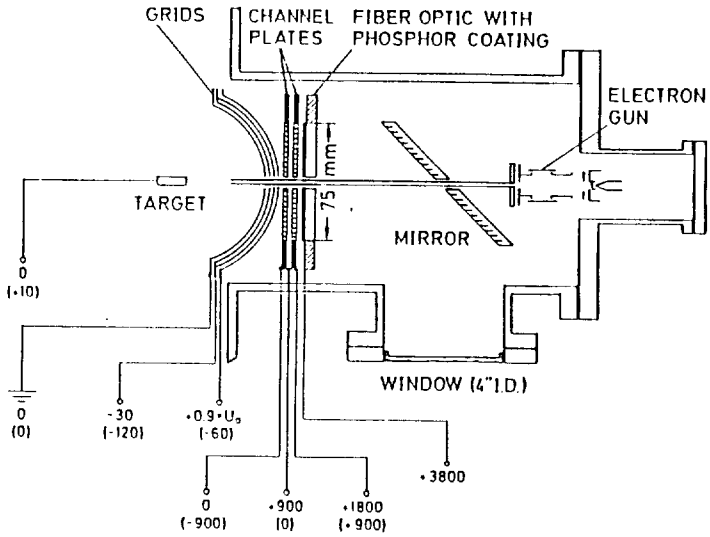

Fig. VIII.2. Schematic of a low-current optical display for LEED and ESDIAD (electron stimulated desorption ion angular distribution, Panel XIV: Chap. 9). In LEED primary beam currents in the 10^{-10} A range can be used, the channel plates enable amplification of the detected electron currents by factors in the 10^7 range. Typical bias potentials [eV] are also indicated. For ESDIAD the potentials are given in brackets; U_0 is the acceleration (primary) voltage [VIII.1]

Fig. 2.11. Calculated diffraction intensities, I, for one-dimensional scattering models. (*a*) A single atom; (*b*) two atoms with spacing of a; (*c*) N atoms in a row, spacing a; (*d*) several groups of N atoms, each with spacing a but with the distance between the groups being $(N + \frac{1}{2})a$; (*e*) several groups of atoms of varying size but otherwise as for (*d*); (*f*) N atoms randomly distributed over $2N$ sites with regular spacing of a (Henzler, 1977).

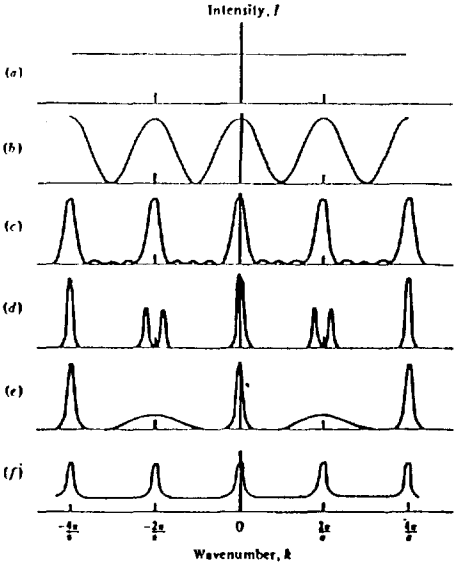

$\Delta\theta \sim \frac{\lambda}{w}$

size of domain.

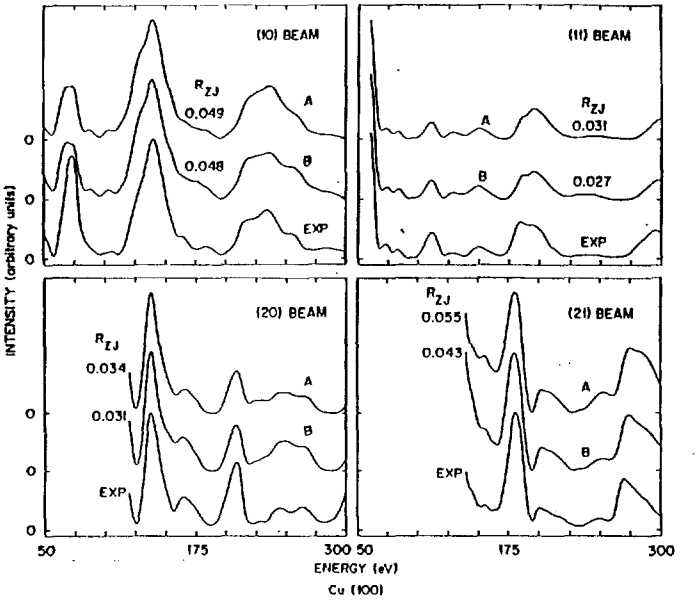

Figure 1.15 LEED current–voltage (I–V) curves for the Cu (100) surface. Each set of curves compares the experimental results with the predictions of a theory which assumes changed interlayer spacing for the top two atomic layers. Curves *A* calculated for $\Delta d_{12} = -0.90\%$ and $\Delta d_{23} = 0.00\%$; Curves *B* calculated for $\Delta d_{12} = -1.45\%$ and $\Delta d_{23} = 2.25\%$. (Source: H.L. Davis and J.R. Noonan, *J. Vac. Sci. Technol.* 1982; 20:842. Reprinted with permission.)

Reflection High Energy Electron Diffraction (RHEED)

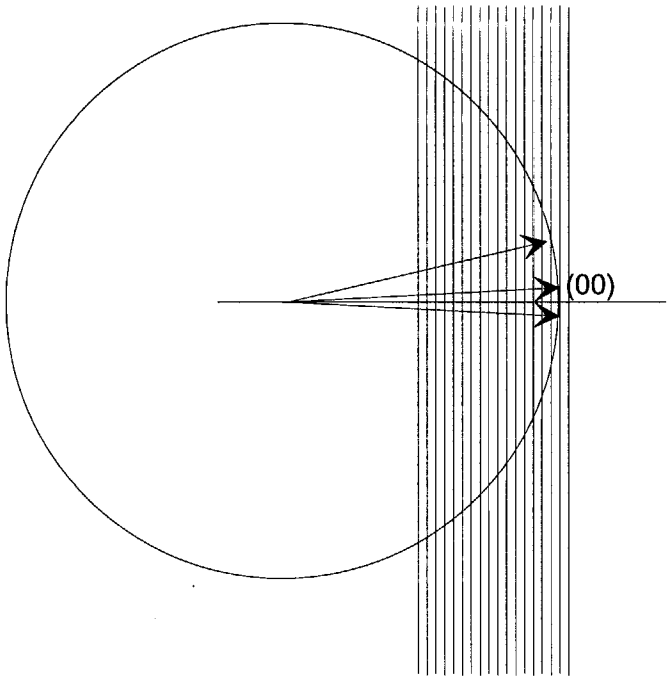

Ewald construction

5-100 keV electrons

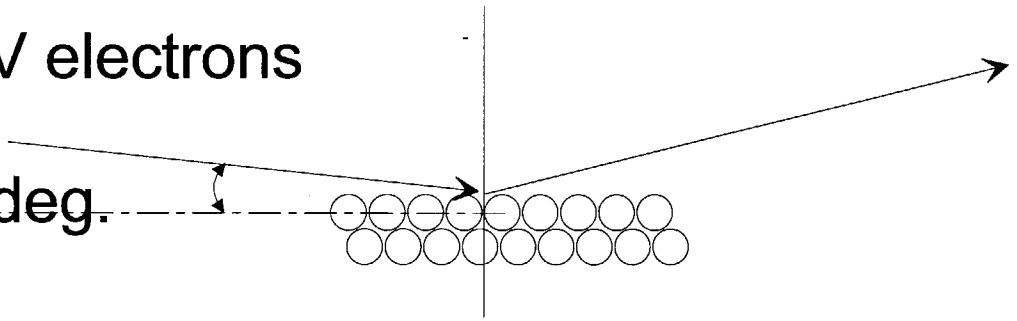

α = 2-5 deg.

Sampling depth is
electron attenuation length x sin α

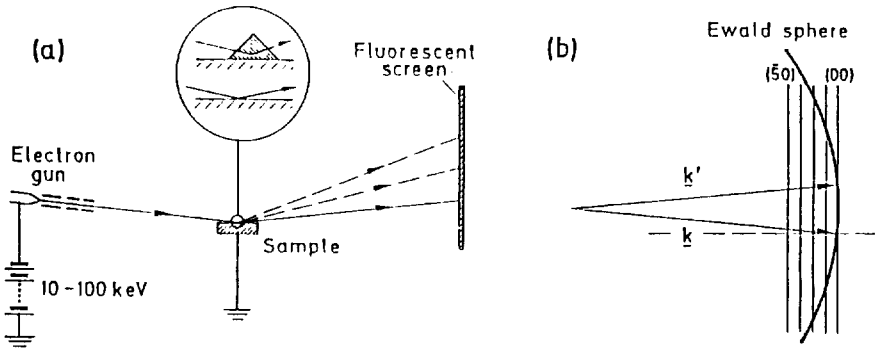

Fig. VIII.4. (a) Schematic of the experimental set-up for RHEED. The inset shows two different scattering situations on a highly enlarged surface area: surface scattering on a flat surface (below) and bulk scattering by a three-dimensional crystalline island on top of the surface (above). (b) The Ewald sphere construction for RHEED. **k** and **k'** are primary and scattered wavevectors, respectively. The sphere radius $k = k'$ is much larger than the distance between the reciprocal lattice rods (hk). For more details, see Sect.4.2 and Figs.4.2,3

REFLECTION HIGH-ENERGY ELECTRON DIFFRACTION (RHEED)

- Uses typically 5 - 100 keV electron guns
- Electron inelastic mean free path L at these energies is about 100 - 1000 Å but sampling depth shallow due to glancing angle.
- Elastic scattering is strongly forward peaked.
- Method simpler than LEED in that it does not require grids and the beam does not need to be accelerated into the phosphor.
- Only useful for very smooth and flat surfaces.
- RHEED is in general not quantitative.
- Roughness: electrons go through asperities and produce "bulk-type" electron diffraction (one-half, pattern is bound by a "shadow edge" parallel to the surface.
- RHEED requires rotation of sample. Changes in periodicity in plane of incidence are not seen.
- Width of spots, which give streaks, not well understood.

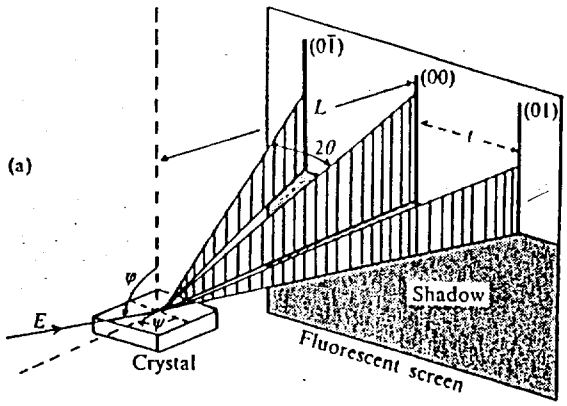

Streaks

Fig. 2.29. RHEED pattern of a GaAs (100) surface along the [$\bar{1}$10] azimuth at 15 keV taken during MBE in an As_4 flux (courtesy J. H. Neave and B. A. Joyce, Philips Research Laboratories).

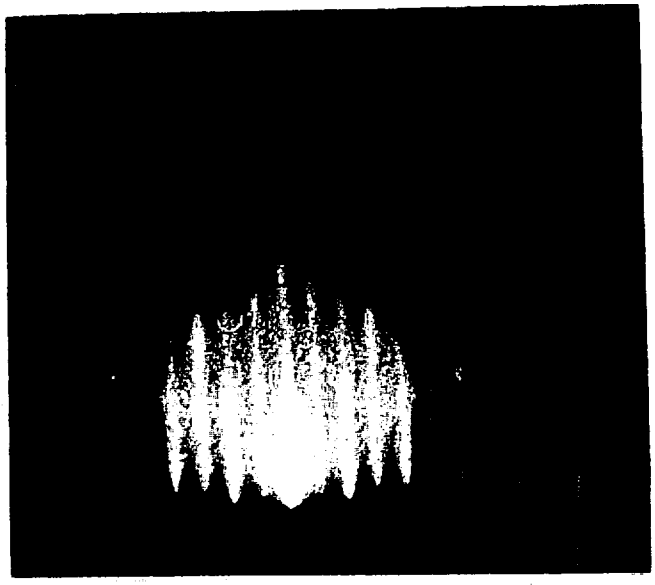

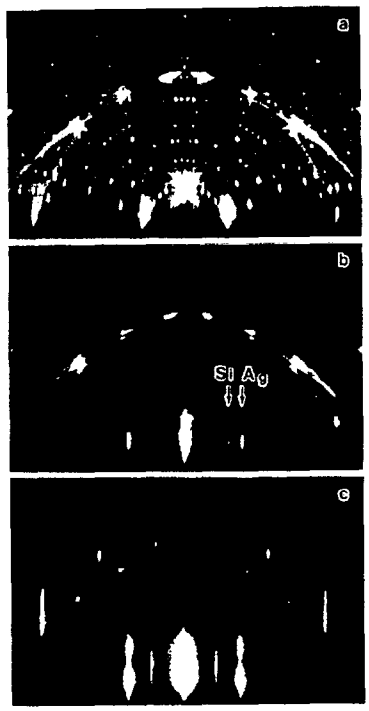

Fig. VIII.5a-c. RHEED patterns taken with a primary energy of E = 15 keV and a direction of incidence of [112] on a Si(111) surface: (a) Clean Si(111) surface with a (7× 7) superstructure. (b) After deposition of nominally 1.5 monolayers (ML) of Ag streaks due to the Ag layers are seen on the blurred (7× 7) structure. (c) After deposition of 3ML of Ag the texture structure due to the Ag layers develops in place of the (7× 7) structure [VIII.3]

RHEED Oscillations

RHEED used typically in growth by MBE (Molecular beam epitaxy)

In MBE, the oscillations of RHEED specular intensities are used to monitor the growth of the layers. Defects scatter electrons off the specular direction producing a drop in the intensity.

As growth continues, the number of steps on the surface increases and the intensity is damped. A method of MBE is to find growth conditions that will give minimum damping.

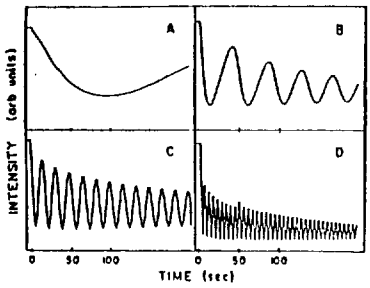

Fig. 12.4. Observed oscillations on a GaAs crystal for increasing flux rates. In *A* the flux is so slow that the substrate steps can scavenge the adatoms before nucleation. The vicinal angle is 1.0 mrad (after [12.10])

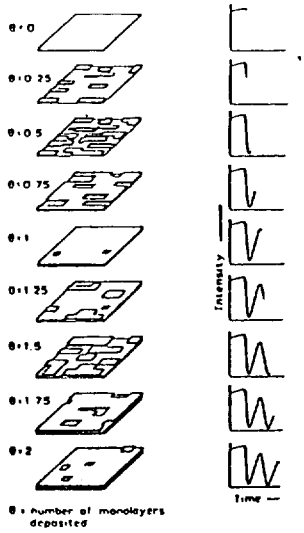

Surface EXAFS

Extended
X-Ray
Absorption
Fine Structure

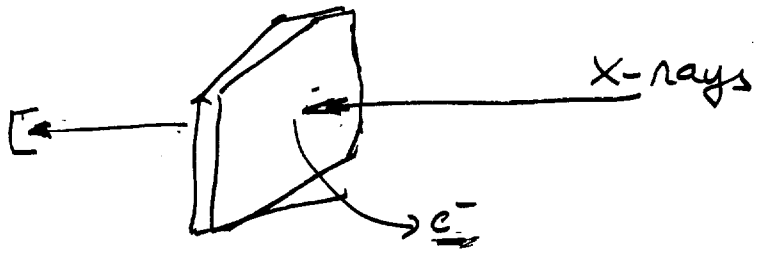

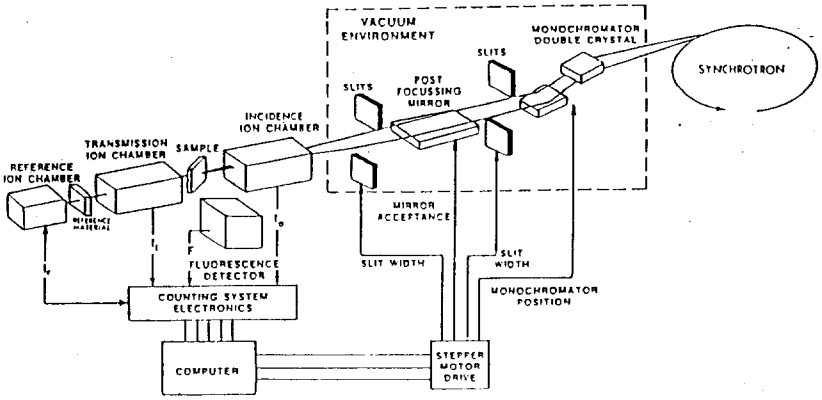

Schematic view of a typical EXAFS experiment at a synchrotron radiation facility. Note that it is possible to record transmission and fluorescence EXAFS simultaneously with reference EXAFS.

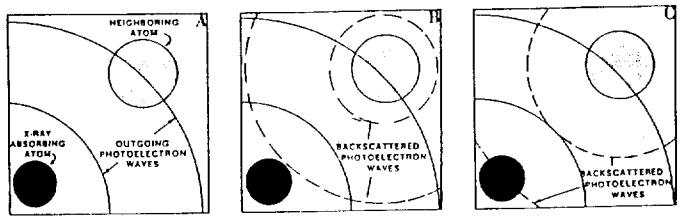

Figure 3 Schematic illustration of the EXAFS phenomenon: (A) outgoing photoelectron (solid curve) from X-ray absorbing atom; (B) destructive interference at the absorbing atom between outgoing (solid curve) and backscattered (dashed curve) photoelectron from neighboring atom; (C) constructive interference at the absorbing atom between outgoing (solid curve) and backscattered (dashed curve) photoelectron from neighboring atom. Adapted from T. M. Hayes and J. B. Boyce. *Solid State Phys.* 37, 173, 1982.

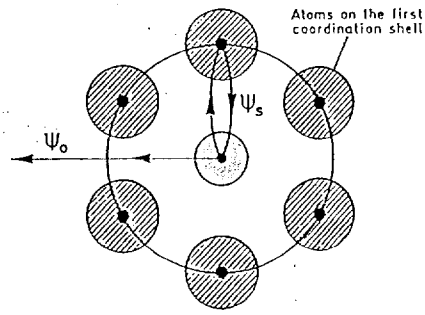

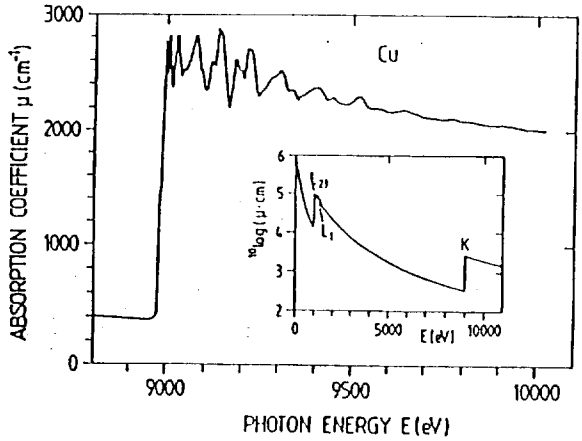

Fig. VII.1. K-shell X-ray absorption coefficient μ of Cu versus X-ray photon energy. Insert: qualitative overview of the absorption coefficient $\mu(\hbar\omega)$ for a wide range of photon energies covering two L edges and one K edge [VII.5]

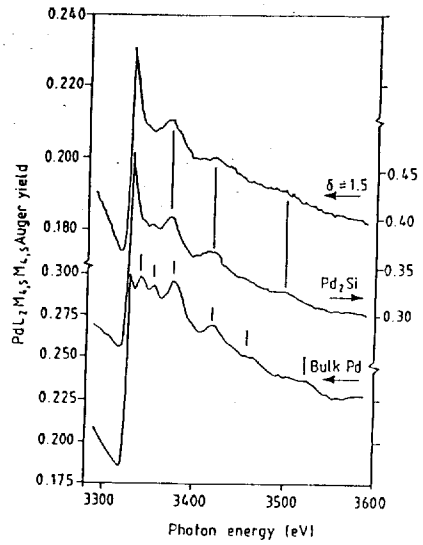

Figure 2 Surface EXAFS spectra above the Pd L_2-edge for a 1.5 monolayer evapor film of Pd on Si(111) and for bulk palladium silicide, Pd_2Si and metallic Pd

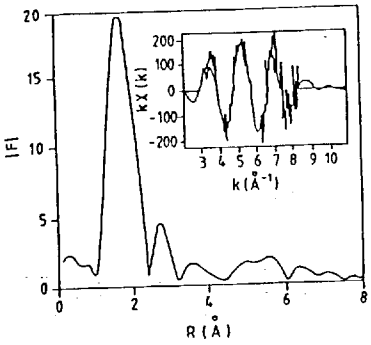

Figure 3 The modulus of the Fourier transform of the SEXAFS spectrum for the half monolayer coverage on Ni(100) The SEXAFS spectrum itself is shown in the inset with the background removed.

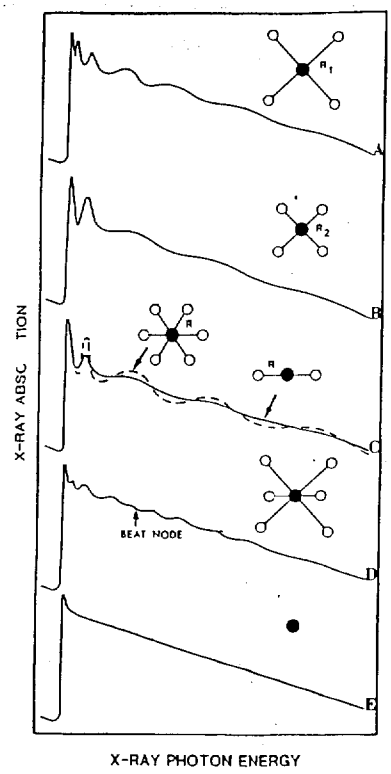

Descriptive aspects of EXAFS: Curves A–E are discussed in the text. Adapted from J. Stohr. In: *Emission and Scattering Techniques: Studies of Inorganic Molecules, Solids, and Surfaces.* (P. Day, ed.) Kluwer, Norwell, MA, 1981.